Hindawi Publishing Corporation
International Journal of Optics
Volume 2012, Article ID 786295, 10 pages
doi:10.1155/2012/786295

Research Article

Lidar Observations of Aerosol Disturbances of the Stratosphere over Tomsk (56.5°N; 85.0°E) in Volcanic Activity Period 2006–2011

Oleg E. Bazhenov, Vladimir D. Burlakov, Sergey I. Dolgii, and Aleksey V. Nevzorov

V.E. Zuev Institute of Atmospheric Optics, Siberian Branch, Russian Academy of Sciences, 1, Academician Zuev square, Tomsk 634021, Russia

Correspondence should be addressed to Aleksey V. Nevzorov, nevzorov@iao.ru

Received 28 October 2011; Accepted 23 December 2011

Academic Editor: Wonho Jhe

The lidar measurements (Tomsk: 56.5°N; 85.0°E) of the optical characteristics of the stratospheric aerosol layer (SAL) in the volcanic activity period 2006–2011 are summarized and analyzed. The background SAL state with minimum aerosol content, observed since 1997 under the conditions of long-term volcanically quiet period, was interrupted in October 2006 by series of explosive eruptions of volcanoes of Pacific Ring of Fire: Rabaul (October 2006, New Guinea); Okmok and Kasatochi (July-August 2008, Aleutian Islands); Redoubt (March-April 2009, Alaska); Sarychev Peak (June 2009, Kuril Islands); Grimsvötn (May 2011, Iceland). A short-term and minor disturbance of the lower stratosphere was also observed in April 2010 after eruption of the Icelandic volcano Eyjafjallajokull. The developed regional empirical model of the vertical distribution of background SAL optical characteristics was used to identify the periods of elevated stratospheric aerosol content after each of the volcanic eruptions. Trends of variations in the total ozone content are also considered.

1. Introduction

The optical and microstructure characteristics of the stratospheric aerosol (SA) substantially influence the radiative, dynamical, and chemical processes in the Earth's atmosphere. The natural and anthropogenic factors, which determine the state of the stratospheric aerosol layer (SAL), may have the character of a constant, gradually accumulating effect or a short-term powerful disturbance. The SA effects are most apparent after explosive volcanic eruptions, when sulfur-containing products are injected through the tropopause directly to the stratosphere, where they participate in a number of photochemical reactions to form the sulfuric acid aerosol, whose mass is several orders of magnitude larger than the mass of the background aerosol. In this case, direct measurements record considerable radiation-temperature effects [1, 2]; there are long-term declines in ozone content because heterogeneous chemical reactions on the increased surfaces of aerosol particles convert relatively inert forms of chlorine compounds to more reactive ozone-depleting species [3–5].

In analysis and prediction of different stratospheric changes, it is necessary to determine and identify the periods of increased SA content and to determine and predict the long-term trends of variations in the SA characteristics for different SAL states. These data make it possible to get systematic SAL observations carried out by different methods of ground-based, balloon-sonde, and satellite measurements and, in particular, with the use of lidars. At present, under active debate [6, 7] those are the geoengineering projects that aimed to counteract the global warming through artificial creation of sulfuric acid aerosol layer in the lower stratosphere in order to increase the albedo of the planet and, thereby, decrease the near-surface temperature or keep it at the present-day level. Naturally, implementation of this global and expensive project will require comprehensively studying the different aspects of expedience, feasibility, and predictability of the consequences of the artificial increase in SA content such as through employment of systematic field, SAL observations in the periods when explosive volcanic eruptions with different intensities impact different regions on Earth.

2. Instruments and Methods of the Observations

The lidar measurements of the optical characteristics of the stratospheric aerosols are conducted at V.E. Zuev Institute of Atmospheric Optics, Siberian Branch, Russian Academy of Sciences since 1986 at the sensing wavelength 532 nm. Data of one-frequency sensing are used to retrieve the SAL optical characteristics in a certain height interval H: the vertical profile of the aerosol backscattering coefficient $\beta_\pi^a(H)$ and the scattering ratio $R(H)$, defined as the ratio of the sum of the aerosol and molecular backscattering coefficients to the latter. The method of calibration of lidar signals against the molecular backscattering coefficients is used. The lidar measurement error grows with increase in the sensing height in accordance with decrease of the signal-to-noise ratio at high heights. In our measurements, the $\beta_\pi^a(H)$ and $R(H)$ measurement error varies from 3 to 4% in the height interval 10–20 km, increasing to 6.5% at heights of 30 km.

Recently, the measurements are conducted at the sensing wavelengths 355 and 532 nm, with the former being the third harmonic of the main frequency (1064 nm) of Nd:YAG laser, and the latter being the second harmonic. We use the Nd:YAG laser, model LS-2132T-LBO, LOTIS-TII firm, Minsk. The energy 70 mJ is reached at the wavelength 532 nm, and the energy 40 mJ is reached at the wavelength 355 nm, at the pulse repetition rate 20 Hz. The optical lidar signals are recorded by the receiving telescope, assembled according to Newton scheme on the basis of the mirror with diameter 30 cm. The photoelectron recording of lidar signals is performed in the photocurrent pulse counting mode. The photomultipliers R7206-01 and R7207-01 of HAMAMATSU firm, Japan, are used. The lidar signal is accumulated using 30–50 thousand laser shots, which corresponds to the accumulation time ~(25–50) minutes.

The measured $R(H)$ profiles reflect the altitude distribution of the relative aerosol content and signify well-defined aerosol layers, thus giving the best idea of aerosol stratification. A criterion of increased SA content is that observations exceed $R(H)$ values for background conditions. Background conditions are obtained from multiyear measurements over the period 1997–2006 which was undisturbed by volcanic eruptions. The general pattern of the time dynamics of the stratospheric aerosol loading is provided by time series of long-term variations in the integrated aerosol backscattering coefficient, which we calculated for the height range 15–30 km.

To identify the possible source of aerosol disturbances, we analyze the reports from electronic resources of volcanic observatories about explosive volcanic eruptions and perform the trajectory analysis of air mass transport between the observation point and location of volcano in the height range where aerosol anomalies were recorded. The trajectory analysis of air mass transport in the stratosphere was performed by the method of constructing the forward and backward trajectories with the use of NOAA HYSPLIT MODEL, available at http://www.ready.noaa.gov/.

3. Regional Empirical Model of Background Stratospheric Aerosol

Since 1997, when, according to our lidar measurements, the stratosphere had relaxed after the aerosol disturbance by eruptions products of the Mt. Pinatubo volcano (June 1991), there was a background SAL state over Tomsk [8, 9] under the conditions of long-term volcanically quiescent period (LVQP) with practically zero trend of changes in SA content during ten years until October 2006. This stratospheric state under the LVQP conditions was first studied with the use of the present-day ground-based and satellite means of observations. The work [10] presents a most comprehensive trend analysis of the nonvolcanic component of the stratospheric aerosol for the period 1971–2004. Deshler et al. [10] analyzed the data of *in situ* measurements at Laramie, Wyoming, lidar records at: Garmisch-Partenkirchen, Germany; Hampton, Virginia; Mauna Loa, Hawaii; São José dos Campos, Brazil, and SAGE II measurements. The SAGE II data suggest that, for different heights and different latitude belts, the background state of the stratospheric aerosol was reached in the period between 1997 and 1999. However, on the whole, work [10] singled out three volcanically quiescent periods with the minimal background content of the stratospheric aerosol: 1978–1980, 1988–1991, and 1997–2004 (the time of the paper writing). Deshler et al. conclude that no long-term change in background stratospheric aerosol has occurred over the period 1970–2004.

Continuous time series data of observations in 2000–2005 were used to construct the statistical seasonal models of the vertical distribution of the optical SAL characteristics for the background stratospheric state [11]. In October 2006, LVQP was interrupted by the eruption of Rabaul (Papua New Guinea), a volcano of the tropical belt, whose injection on October 7 reached a height 18 km. This model of background SA was used to analyze the process of development and relaxation of the elevated aerosol content in the stratosphere over Tomsk, which was observed in the fall-winter period of 2006/07. After the Rabaul eruption, the background stratospheric state continued until July 2008. The seasonal model of background SA, supplemented with data of measurements in 2007/08, is presented in Figure 1 in the form of altitude $R(H)$ profiles. The notations "winter" and "summer" in Figure 1 actually mean winter + spring and summer + fall and include, respectively, the months from November to April and from May to October.

This division was selected taking into account the specific features of the atmospheric general circulation and in accordance with the observed mean differences in the aerosol content in these periods. We processed a total of 118 profiles for the winter-spring (November–April) period, and 79 profiles for the summer-fall (May–October) period, each being an average of 2-3 profiles, taken for a single night of measurements. The lidar measurements in the stratosphere, with signals recorded in the photocurrent pulse counting mode, are performed only at nighttime to avoid the background illumination from daytime sky. Hence, there are normally fewer measured profiles in summer than winter period.

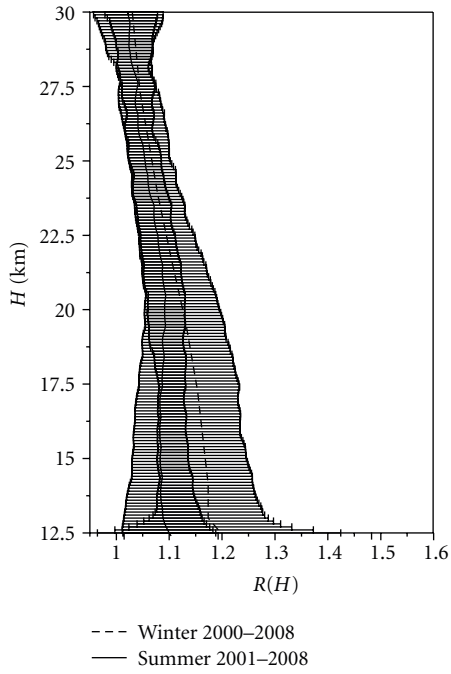

Figure 1: Averaged seasonal profiles of the scattering ratio at the wavelength 532 nm for 2000–2008. The horizontal lines show the corridors of the standard deviation (SD).

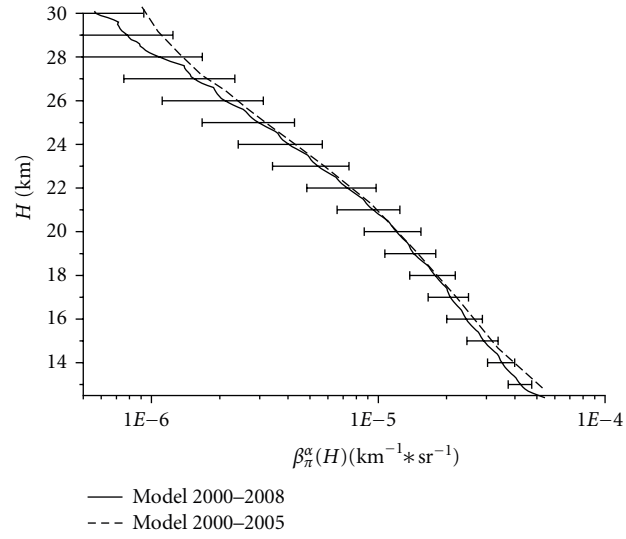

Figure 2: The average background profile of the aerosol backscattering coefficient at the wavelength 532 nm according to measurements in 2000–2005 and 2000–2008. Horizontal lines show the SD corridors for the profile obtained for 2000–2008.

The summer-fall profiles are mainly characterized by vertically uniform aerosol content and are determined by the minimum values $R(H) \sim 1.05$–1.1. Compared to the summer-fall period, in the winter-spring period the aerosol content somewhat increases (with $R(H)$ correspondingly growing to 1.15–1.2) in the lower part of the stratosphere up to heights ~20 km. At the same time, the $R(H)$ profiles coincide within the corridors of the standard deviation (SD) for these two periods. The observed seasonal differences in the content of the midlatitude SA are explained by the fact that, in accordance with stratospheric general circulation models, the meridional stratospheric transport of air masses and aerosol, entrained from the tropical reservoir, to the middle and high latitudes intensifies in the winter-spring period [12]. The dataset of the measurements in 2000–2008 for all seasons was used to create an average background profile of the aerosol backscattering coefficient at the wavelength 532 nm for the midlatitude stratosphere over Tomsk, which is presented in Figure 2.

Here, this profile is compared with our model for the background period 2000–2005. On the whole, the 2000–2005 model is within the SD corridor of the 2000–2008 model. Somewhat larger differences at the altitudes of 26–30 km may be due to larger measurement error, increasing to 6.5% at these altitudes versus 3-4% error at the altitudes of 10–20 km. The empirical model for 2000–2008 in this height interval is well approximated by the function $\beta^{a}_{\pi}(H) = 6.33 \cdot 10^{-4} e^{-0.2 \cdot H} - 7.86 \cdot 10^{-7}$.

The background model was used to determine the periods of elevated SA content after subsequent volcanic eruptions. It is noteworthy that $R(H)$ values, exceeding the SD corridors of the $R(H)$ values of the background model profile for the corresponding season, were considered as a criterion of an elevated SA content.

4. Changes in the Stratospheric Aerosol Content during 2006–2011

The chronology of the volcanic eruptions in 2006–2011, after which elevated SA content was recorded over Tomsk, is presented in Table 1. Characteristically, the first five volcanoes of those listed in the table refer to the belt of volcanic activity, located along the boundaries of the Pacific lithospheric plate, the so-called the Pacific Ring of Fire. Probably, tectonic processes of the same nature caused the volcanic eruptions of the Ring of Fire in 2006–2009 as were responsible for tragic earthquake and tsunami on the Pacific coast of Japan and other countries in March 2011.

The time behavior of the integrated aerosol backscattering coefficient B^{a}_{π}, determined from the sensing data at the wavelength 532 nm, is shown in Figure 3. Here, each point represents the data, averaged over ten days of measurements. There are periodic bursts of elevated aerosol content after every volcanic eruption. The increasing trend of SA content (B^{a}_{π} value) for the volcanic activity period 2006–2011 was statistically significant and equaled (6.7 ± 0.2) % per year.

When analyzing the probability of propagation of volcanic eruption products to a specific observation point, it should be remembered that, usually the products erupted in the tropical belt later spread around the globe, products erupted at midlatitudes spread throughout the hemisphere where the eruption occurred, and products erupted at high latitudes are carried predominately by polar transport to

Table 1: Chronology of volcanic eruptions, whose traces were recorded in the stratosphere over Tomsk in 2006-2011.

Name	Latitude	Longitude	Date	Period of aerosol disturbance of the stratosphere
Rabaul, Papua New Guinea	4.3°S	152.2°E	6 Oct 2006	late October 2006–winter 2006/07
Okmok, Aleutian Islands	53.4°N	168.1°W	12 Jul 2008	late July—fall of 2008
Kasatochi, Aleutian Islands	52.2°N	175.5°W	6–8 Aug 2008	
Redoubt, Alaska	60.5°N	152.7°W	18 Mar–4 Apr 2009	April-May 2009
Sarychev Peak, Kuril Islands	48.1°N	153.2°E	11–16 Jun 2009	July–December 2009
Eyjafjallajokull, Iceland	63.6°N	19.6°W	14 Apr 2010	Minor disturbance of the lower stratosphere in late April 2010
Grimsvötn, Iceland	64.4°N	17.3°W	21 May 2011	Second half-year of 2011

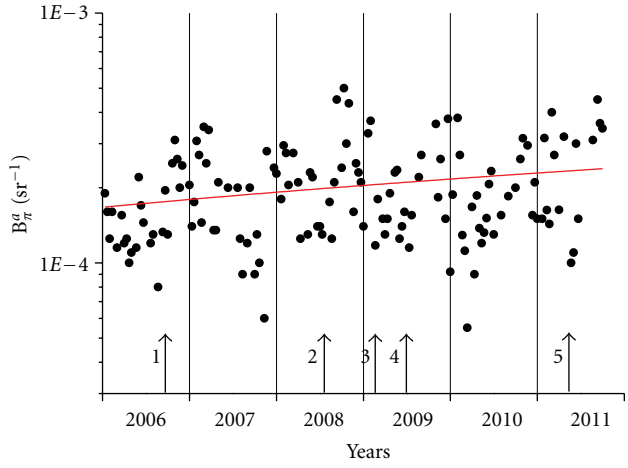

Figure 3: The dynamics of changes in the integrated aerosol backscattering coefficient in the height range 15–30 km over Tomsk in 2006–2011. Straight line shows the increasing trend. Arrows indicate the volcanic eruptions: Rabaul (1); Okmok and Kasatochi (2); Redoubt (3); Sarychev Peak (4); Grimsvötn (5).

the corresponding polar region. Moreover, the propagation speed of eruption products from volcanoes of the tropical belt depends on the season and phase of the quasi-biennial oscillation (QBO) of zonal winds in the equatorial stratosphere. The transport from the tropical reservoir to the middle and high latitudes is enhanced in the winter period and in the QBO westerly phase [12]. After eruption of the tropical-belt volcano Rabaul, a rapid and well-apparent (in Tomsk) increase in the aerosol loading of the lower stratosphere was observed as soon as 10 days later and had persisted until early spring of 2007. A favorable fact was that the time of eruption and the subsequent period were characterized by the QBO westerly phase of the zonal tropical wind.

In July-August 2008, the background SAL state was again interrupted by explosive eruptions of Okmok and Kasatochi midlatitude volcanoes on Aleutian Islands. Figure 4 shows examples of the altitude profiles of the scattering ratio $R(H)$, which were recorded after the eruptions of Rabaul, Okmok, and Kasatochi volcanoes. The profiles reflect the relative content and altitude stratification of aerosols.

Figure 5 presents an example of air mass back trajectory in the stratosphere from Tomsk (height 15.5 km), where we observed well-defined aerosol layer on August 8, 2008 (see Figure 4). The trajectory is presented for two successive time intervals (Figures 5(a) and 5(b)). The trajectory analysis shows that, on August 8, the air masses arrived at Tomsk from the region of Aleutian Islands, where Okmok volcano is located, and where its eruption products spread after July 12. An analogous analysis was also performed for observations of aerosol layers from other volcanoes.

After eruptions of Okmok and Kasatochi volcanoes, the aerosol disturbance of the stratosphere was observed at the observation sites in Minsk (53.9°N; 27.4°E), Tomsk, and Vladivostok (43.0°N; 131.9°E) at lidar network CIS-LiNet for monitoring aerosol and ozone in CIS regions until late 2008. The results of these measurements, as well as the results of expedition measurements, performed by Institute of Atmospheric Optics in Gobi Desert, were considered in detail in [13], together with the air mass trajectory analysis.

In spring of 2009, aerosol layers were again observed in the stratosphere over Tomsk (Figure 6) after a series of eruptions of Redoubt volcano in March-April 2009. We observed a general increase of the aerosol content in the lower stratosphere; at the sensing wavelength 532 nm the R values increased to 1.3-1.4 versus the background values 1.1–1.15. It is noteworthy that well-defined aerosol layers at heights ~(14–16) km were observed on May 6, 2009.

The background state, characterized by the values $R \sim 1.1$, was again observed in June 2009. Well-defined aerosol layers subsequently formed at heights 13–17 km (Figure 7). These layers were due to eruption of Sarychev Peak volcano in the Kuril Islands; it occurred on June 12–16 and injected the eruption products up to the height 16 km. Traces of eruption of this volcano were observed practically until late 2009. In contrast to aerosol layers due to previous volcanoes, whose passage over Tomsk was discontinuous in character, in August-September 2009 there was stable aerosol stratification; the profiles of the scattering ratio for August are presented in Figure 7.

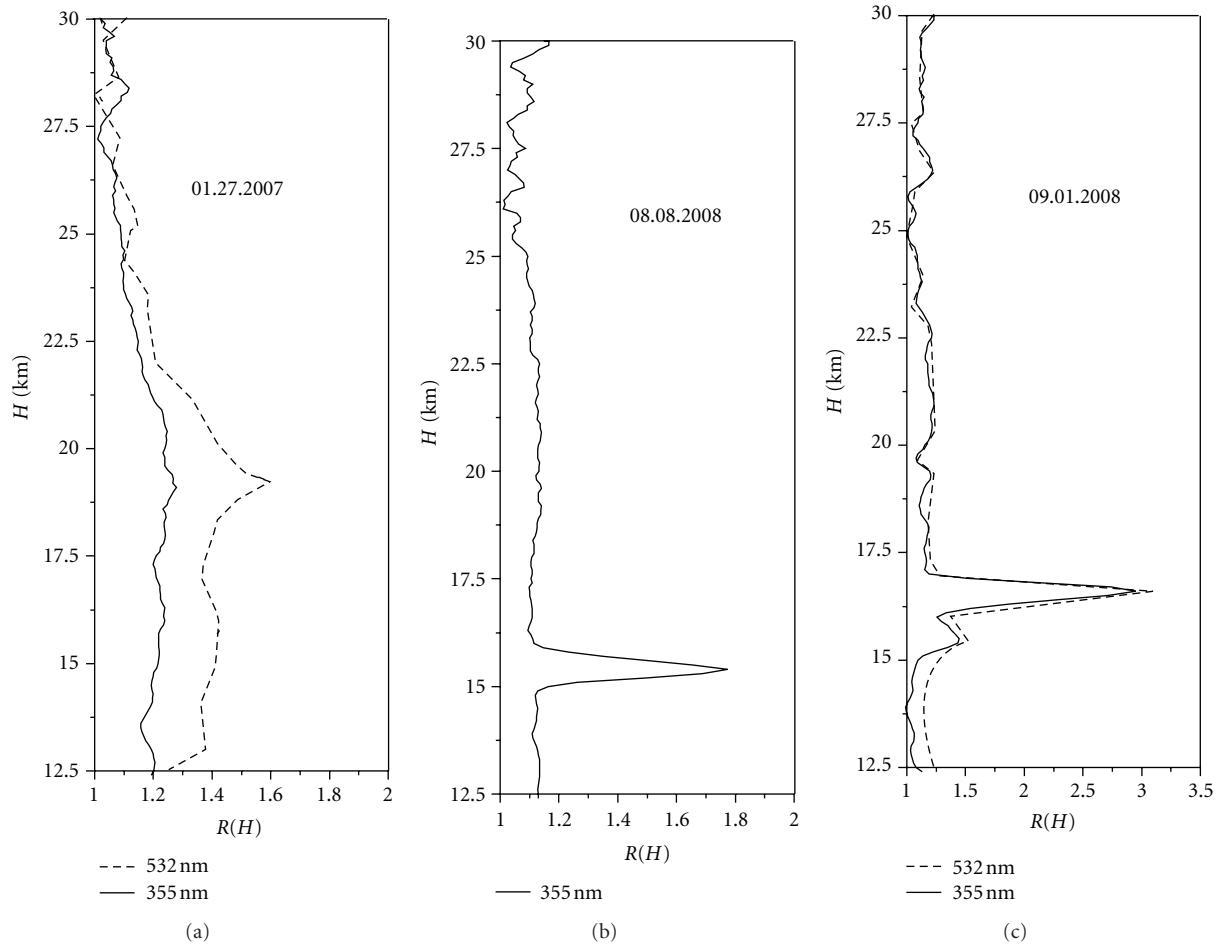

Figure 4: Examples of altitude $R(H)$ profiles in the stratosphere over Tomsk after eruptions of Rabaul, Okmok, and Kasatochi volcanoes. The measurements were performed on January 27, 2007; August 8, 2008; September 1, 2008.

The stratospheric aerosol disturbances, caused by the volcanic eruptions in 2006–2009, were recorded in Cloud-Aerosol Lidar and Infrared Pathfinder Satellite Observations (CALIPSO), at the observation sites of European Aerosol Research Lidar Network (EARLINET) and at some other lidar observatories [14–17].

In late April 2010, there were aerosol anomalies in the atmosphere over Tomsk, associated with the transport of eruption products of Eyjafjallajokull volcano, Iceland (April 14, 2010). First traces of the eruption were recorded in the troposphere over Tomsk on April 19. Well-defined aerosol layers were observed at heights 3–6 km. On the whole, the volcanic aerosol persisted in the troposphere until late April; however, it penetrated the stratosphere insignificantly and, hence, had no marked long-term radiation-temperature effects.

On the whole, during 2010 and in the first half of 2011, there was a background SAL state in the stratosphere. On May 21, 2011, Grimsvötn volcano erupted in Iceland and injected eruption products to the height higher than 20 km. Background SA content was still observed in Tomsk in June. In August-September, anomalous aerosol values were recorded in the lower stratosphere, with aerosol maximum at heights 14–18 km (Figure 8). The trajectory analysis of air mass transport in the stratosphere shows that the aerosol layers observed may be associated with the transport of eruption products of Grimsvötn volcano. Data, reported by personnel of lidar observatory at Institute of Physics, Belarus National Academy of Sciences, indicate that aerosol layers were also observed at analogous heights over Minsk (53.9° N, 27.6° E) from summer to September 2011.

5. Stratospheric Aerosol and Trends of Variations in the Total Ozone Content

The total ozone (TO) content, recorded by the present-day ground-based and satellite means of measurements, had considerably decreased from early 1980s to mid 1990s. The decline until mid 1990s has been conventionally attributed to the chemical ozone destruction due to increasing concentrations of ozone-depleting substances (ODSs) in the stratosphere. From the second half of 1990s to the present, the destruction of ozone layer has stopped almost everywhere

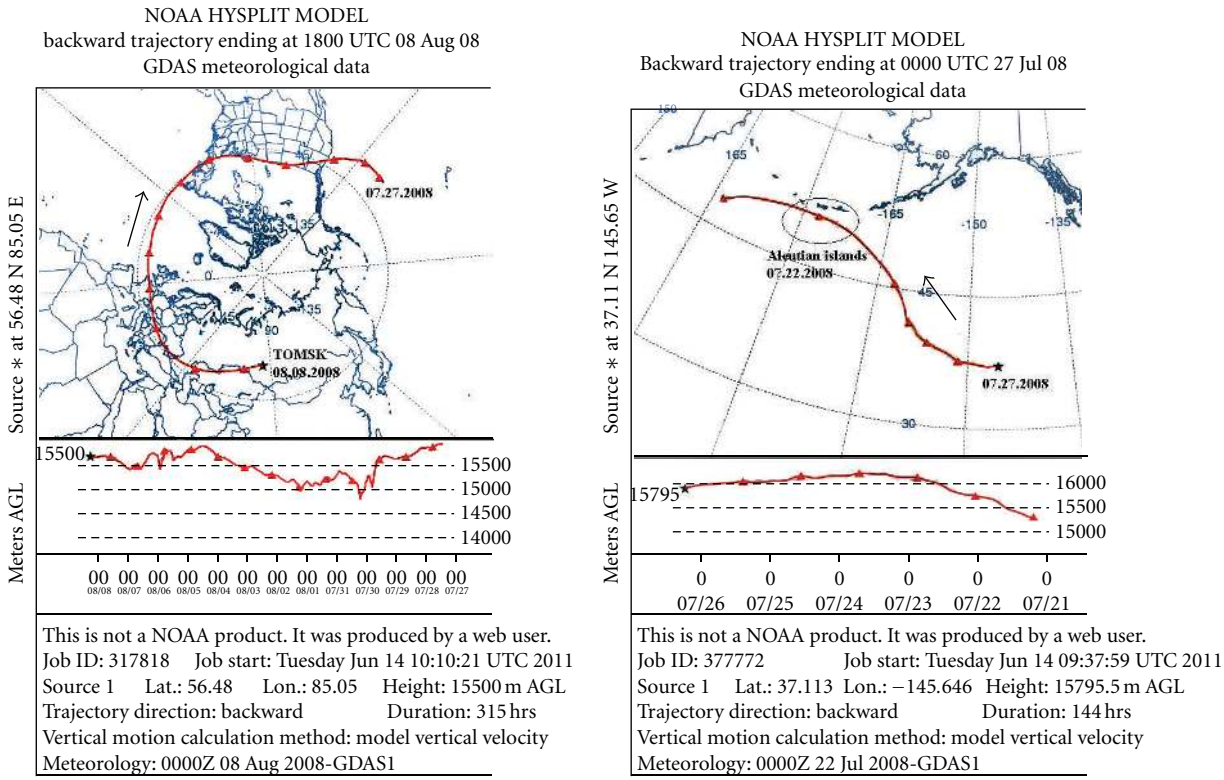

(a) (b)

Figure 5: Air mass back trajectories starting at Tomsk (height 15.5 km) for the measurement time 1800 UTC on August 8, 2008; (a) beginning of the trajectory and (b) continuation of the trajectory.

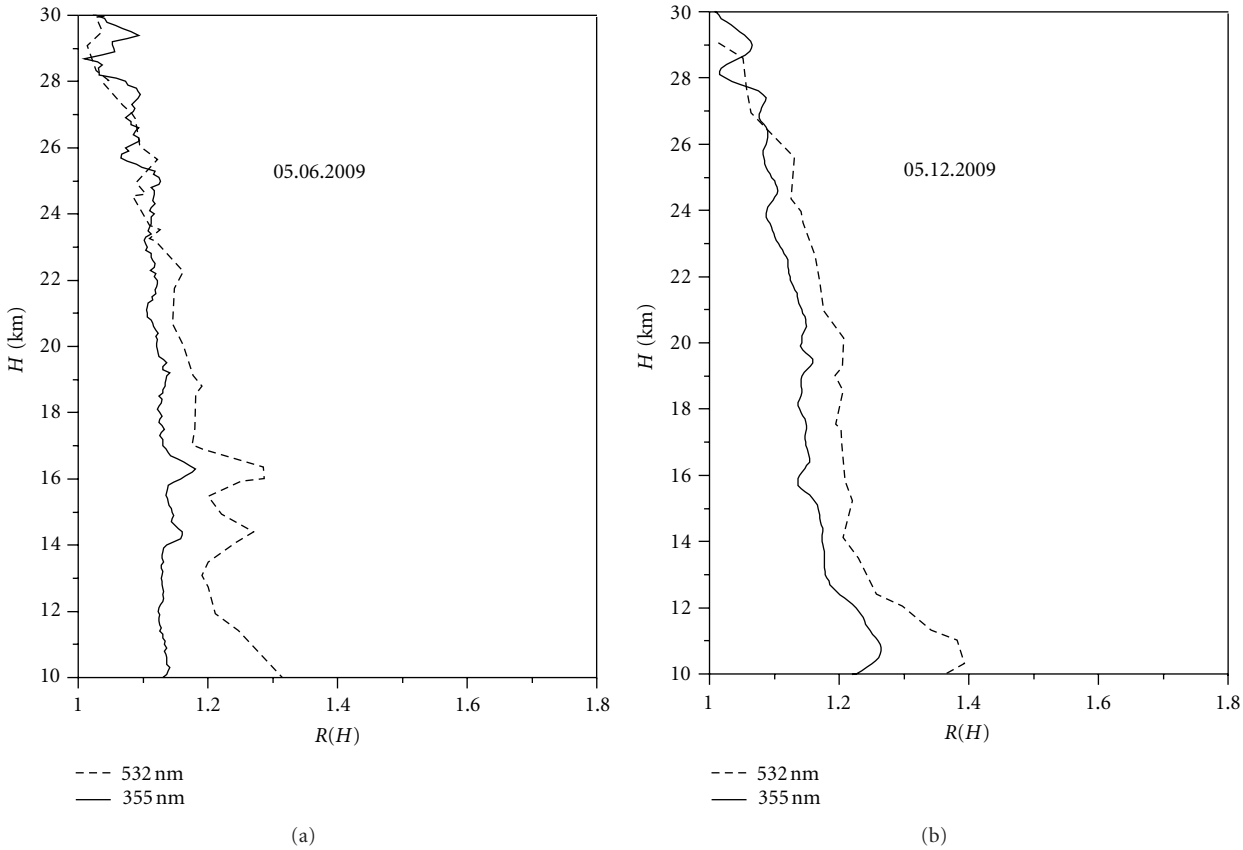

(a) (b)

Figure 6: Altitude profiles $R(H)$ over Tomsk in May 2009.

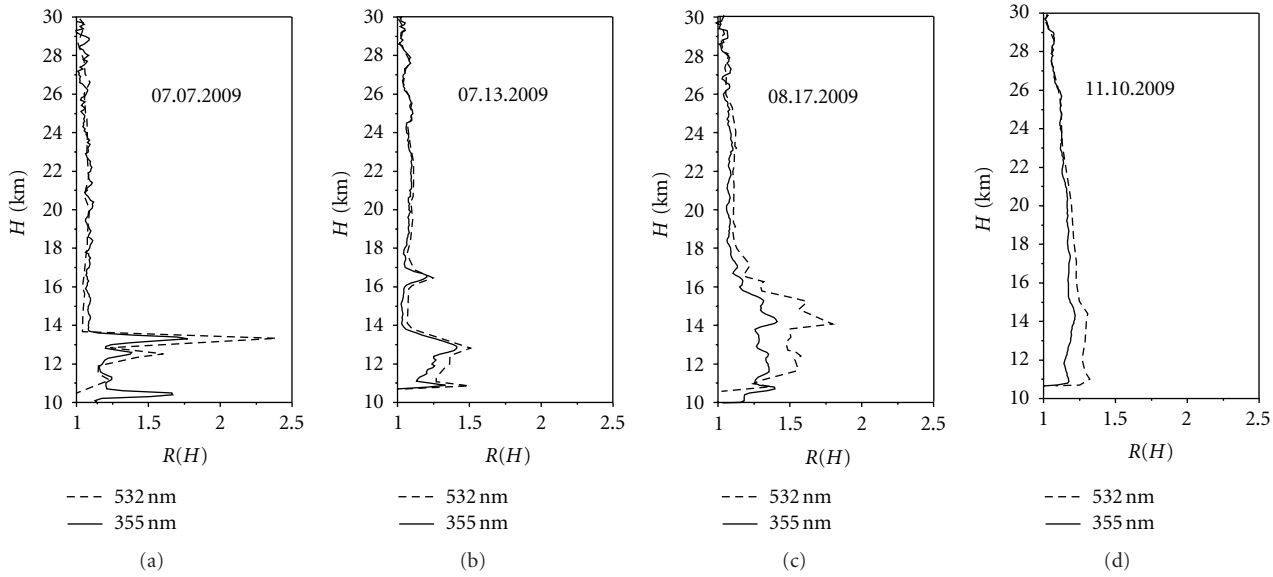

Figure 7: The altitude profiles $R(H)$ over Tomsk in July-November 2009.

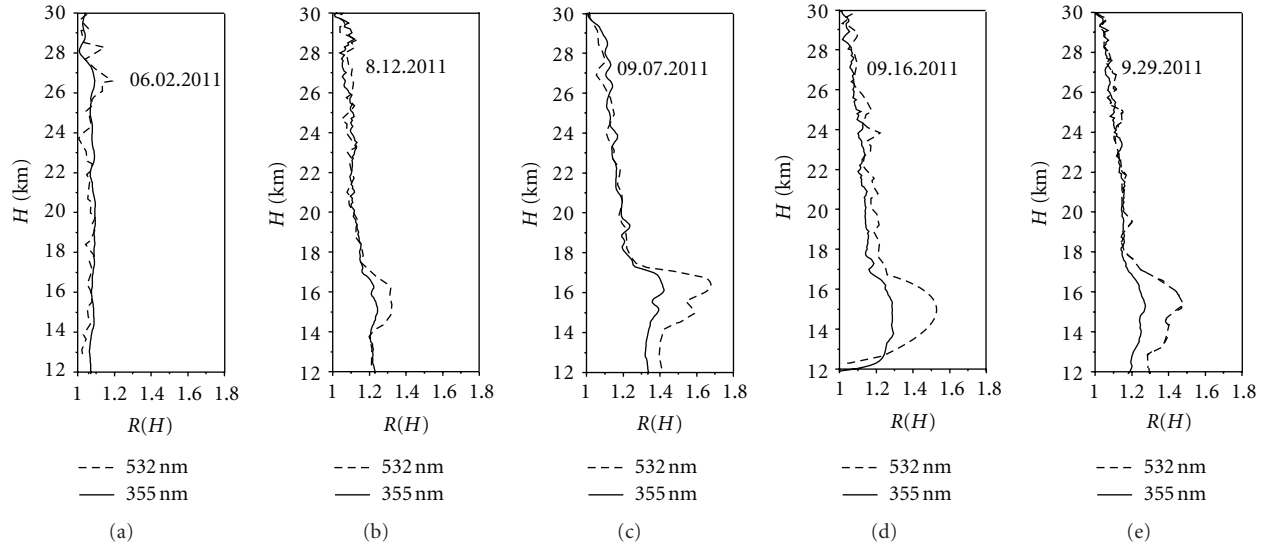

Figure 8: Altitude profiles $R(H)$ over Tomsk in June–September 2011.

[18–20] or an increasing ozone trend becomes apparent, especially at the Northern Hemisphere middle to high latitudes. Simultaneously, with the TO stabilization and growth, there are signs for the stabilization and reduction of the equivalent effective stratospheric chlorine (EESC), which characterizes the ODS concentration and had grown until about 1996. The tendency toward stabilization and reduction is preferably related to implementation of United Nations Montreal protocol and its subsequent Amendments, which came into force in 1989 and stated that production and emission of ODS to the atmosphere should be reduced.

However, attribution of ozone trend just to ODS changes is not a unique problem because of many factors making their own contribution to ozone trends and variations, for example, at midlatitudes. Ozone researchers usually single out and consider the following main factors that may have the character of short- or long-term natural and anthropogenic impact: chemical atmospheric processes, atmospheric dynamics, temperature-climate changes, solar activity, and volcanic disturbances of the stratosphere. These processes, in turn, are interrelated to some or another degree, and strengthening or weakening of one factor may alter the degree of impact of some other factor and, ultimately, the ozone changes in specific regions. The processes of ozone recovery depend essentially on the temperature and intensity of stratospheric transport and on overall climate changes, which had been modified considerably since 1980s such as due to the growth of greenhouse gas concentrations [21–27].

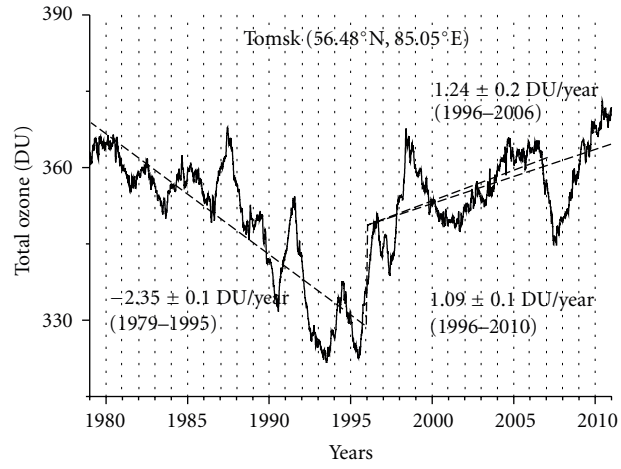

Figure 9: The time series of the total ozone content for Tomsk; the curve is plotted using satellite data (until 1993) and M-124 ozonometer data (1994–2010). The dashed lines show the linear trends for the corresponding time periods.

There is no doubt that elevated stratospheric aerosol content after explosive volcanic eruptions affects the TO level [3–5, 28]. The record low TO content in 1992-1993 had coincided in time with the period of maximum aerosol pollution of the stratosphere by eruption products of Pinatubo volcano. The TO stabilization and growth starting from the second-half of 1990s was time coincident with the minimum background SA content that was observed from 1997 to 2006 under the conditions of long-term volcanically quiescent period.

Figure 9 presents the time series of TO content over Tomsk for period 1979–2010. It was plotted using measurements by TOMS instruments on Nimbus 7 (1979–1992) and Meteor (1993) satellites [29], as well as ground-based spectrophotometric measurements by M-124 ozonometer (1994–2010) in Institute of Atmospheric Optics, Siberian Branch, Russian Academy of Sciences. Data of satellite and our ground-based measurements well agree to within ~1.1%. The trends were plotted separately for the periods 1979–1995, 1996–2006, and 1996–2010. Before the trend determination, the annual record was processed to remove the seasonal dependence; then annually average value was added. The 365-point smoothing was applied to the time series during plotting.

From Figure 9, it is seen that the time behavior includes two dependences: the negative linear trend of -2.35 ± 0.1 DU/yr for the period 1979–1995 and the positive trend of 1.24 ± 0.2 DU/yr for the period 1996–2006. The trend for the period 1996–2010 is also positive, but decreases to 1.09 ± 0.1 DU/yr. The fact that the positive TO trend for the period 1996–2010 is less than that for the period 1996–2006 may be because stratospheric aerosol, whose content increased due to the activity of volcanoes of the Pacific Ring of Fire, had affected the ozone destruction.

The volcanoes in this series had relatively low intensity (almost two orders of magnitude less intense than Pinatubo volcano, by the mass of sulfur dioxide injected to the stratosphere) and were accompanied by short term (within a few months) increases in SA content. For comparison, the TO decline was observed for a few years after the eruption of Pinatubo volcano, which injected about 17–20 Mt sulfur dioxide to the stratosphere. Rabaul volcano injected about 0.13 Mt sulfur dioxide (as estimated in [30]) to the stratosphere; and Sarychev Peak volcano injected 0.2 Mt to the upper troposphere-stratosphere [15]. Nonetheless, TO changes were insignificant and short-term. For instance, a statistically significant negative correlation between the variations in the stratospheric aerosol and TO contents was observed at the latitude of Tomsk after eruption of Rabaul volcano, in the period of the maximum aerosol disturbance of the stratosphere in January–February 2007 [5]. These short-term TO changes had no effect on the general increasing TO trend until 2010, but the growth rate decreased.

Signs of the TO stabilization and growth may be due to (1) implementation of the Montreal protocol, (2) the minimal SA content since 1997, or (3) climate change. The relative contributions of these factors are not well established. Nevertheless, it is necessary to make prognostic estimates regarding possible effects of additional aerosol of natural or anthropogenic origin on the state of the Earth's ozone layer. Since the ozone layer acts as a natural shield for the earth's biosphere against shortwave UV solar radiation, better understanding of the effect of changing aerosol on ozone is imperative.

6. Conclusion

Data of regular lidar observations of the stratospheric aerosol layer at midlatitudes of Tomsk were used to identify the periods of elevated aerosol content in the stratosphere; these events are associated with explosive eruptions of volcanoes of Pacific Ring of Fire: Rabaul (October 2006), Okmok (July 2008), Kasatochi (August 2008), Redoubt (March-April 2009), Sarychev Peak (June 2009), and Grimsvötn (May 2011). The maximum values of the integrated aerosol backscattering coefficient of the stratosphere reached $(4\text{-}5)\cdot 10^{-4}\,\mathrm{sr}^{-1}$ in the periods of elevated SA content versus the average values $\sim 1.5\cdot 10^{-4}\,\mathrm{sr}^{-1}$ for the background period 1997–2006, which did not exceed $2.5\cdot 10^{-4}\,\mathrm{sr}^{-1}$ even in the winter periods of the maximum aerosol content. The increasing TO trend for the period 1996–2010, which includes the above-mentioned periods of elevated aerosol content, flattened as compared to the increasing trend for the period of minimum background SA content in 1996–2006. The background state of the stratospheric aerosol layer, which had been observed from 1997 to September 2006 under the conditions of long-term volcanically quiet period, was interrupted, which should be taken into consideration during analysis of the variability trends of the background component of the stratospheric aerosol and stratospheric changes as a whole.

Acknowledgments

This work was supported by the Ministry of Education and Science of the Russian Federation (state Contracts nos. 02.740.11.0674, 14.740.11.0204, and 16.518.11.7067) and by the Presidium of Siberian Branch of Russian Academy of Sciences (project no. 2).

References

[1] M. P. McCormick, L. W. Thomason, and C. R. Trepte, "Atmospheric effects of the Mt Pinatubo eruption," *Nature*, vol. 373, no. 6513, pp. 399–404, 1995.

[2] K. Labitzke and M. P. McCormick, "Stratospheric temperature increases due to Pinatubo aerosols," *Geophysical Research Letters*, vol. 19, no. 2, pp. 207–210, 1992.

[3] D. J. Hofmann and S. Solomon, "Ozone destruction through heterogeneous chemistry following the eruption of El Chichon," *Journal of Geophysical Research*, vol. 94, no. 4, pp. 5029–5041, 1989.

[4] A. Ansmann, F. Wagner, U. Wandinger et al., "Pinatubo aerosol and stratospheric ozone reduction: observations over central Europe," *Journal of Geophysical Research D*, vol. 101, no. 13, pp. 18775–18785, 1996.

[5] V. V. Zuev, O. E. Bazhenov, V. D. Burlakov, M. V. Grishaev, S. I. Dolgii, and A. V. Nevzorov, "On the effect of volcanic aerosol on variations of stratospheric ozone and NO_2 according to measurements at the Siberian Lidar Station," *The Atmospheric and Oceanic Optics*, vol. 21, no. 11, pp. 825–831, 2008.

[6] B. Kravitz, A. Robock, L. Oman, G. Stenchikov, and A. B. Marquardt, "Sulfuric acid deposition from stratospheric geoengineering with sulfate aerosols," *Journal of Geophysical Research D*, vol. 114, no. 16, Article ID D16119, 7 pages, 2010.

[7] A. Robock, L. Oman, and G. L. Stenchikov, "Regional climate responses to geoengineering with tropical and Arctic SO_2 injections," *Journal of Geophysical Research D*, vol. 113, no. 16, Article ID D16101, 2008.

[8] V. V. Zuev, V. D. Burlakov, A. V. El'nikov, A. P. Ivanov, A. P. Chaikovskii, and V. N. Shcherbakov, "Processes of long-term relaxation of stratospheric aerosol layer in Northern Hemisphere midlatitudes after a powerful volcanic eruption," *Atmospheric Environment*, vol. 35, no. 30, pp. 5059–5066, 2001.

[9] V. V. Zuev, O. E. Bazhenov, V. D. Burlakov, and A. V. Nevzorov, "Long-term trends, seasonal and anomalous short-term variations of background stratospheric aerosol," *Atmospheric and Oceanic Optics*, vol. 21, no. 1, pp. 33–38, 2008.

[10] T. Deshler, R. Anderson-Sprecher, H. Jäger et al., "Trends in the nonvolcanic component of stratospheric aerosol over the period 1971–2004," *Journal of Geophysical Research D*, vol. 111, no. 1, Article ID D01201, 2006.

[11] V. V. Zuev, V. D. Burlakov, A. V. El'nikov, and A. V. Nevzorov, "Lidar observations of midlatitude stratospheric aerosol layer during long-term volcanically quiet period," *Atmospheric and Oceanic Optics*, vol. 19, no. 7, pp. 535–539, 2006.

[12] M. H. Hitchman, M. McKay, and C. R. Trepte, "A climatology of stratospheric aerosol," *Journal of Geophysical Research D*, vol. 99, no. 10, pp. 20689–20700, 1994.

[13] V. V. Zuev, S. BalinYu, O. A. Bukin et al., "Results of joint observations of aerosol perturbations in the stratosphere at stations of CIS-LiNet in 2008," *Atmospheric and Oceanic Optics*, vol. 22, no. 5, pp. 450–456, 2009.

[14] B. G. Martinsson, C. A. M. Brenninkmeijer, S. A. Cam et al., "Influence of the 2008 Kasatochi volcanic eruption on sulfurous and carbonaceous aerosol constituents in the lower stratosphere," *Geophysical Research Letters*, vol. 36, no. 12, Article ID L12813, 2009.

[15] G. D'Amico, A. Amodeo, A. Boselli et al., "Stratospheric aerosol layers over southern Italy during the summer of 2009: lidar observations and model comparison," in *Proceedings of the 25th International Laser Radar Conference*, vol. 1, pp. 473–476, St.-Petersburg, July 2010, month year.

[16] I. Mattis, P. Seifert, D. Muller et al., "Volcanic aerosol layers observed with multi-wawelength Raman lidar over Europe since summer 2008," in *Proceedings of the 25th International Laser Radar Conference*, vol. 1, pp. 445–448, St.-Petersburg, July 2010.

[17] T. Trickl, H. Giehl, H. Jäger, and M. Fromm, "33 years of stratospheric aerosol measurements at Garmisch-Partenkirchen (1976–2010)," in *Proceedings of the 25th International Laser Radar Conference*, vol. 1, pp. 465–468, St.-Petersburg, July 2010.

[18] E. C. Weatherhead and S. B. Andersen, "The search for signs of recovery of the ozone layer," *Nature*, vol. 441, no. 1, pp. 39–45, 2006.

[19] World Meteorological Organization (WMO), "United nations environment programme (UNEP): scientific assessment of ozone depletion: 2006," Tech. Rep. 50, World Meteorological Organization, Global Ozone Research and Monitoring Project, Geneva, Switzerland, 2007.

[20] World Meteorological Organization, "Global ozone research and monitoring project," type 52, Scientific Assessment of ozone Depletion: 2010 Pursuant to Article 6 of the Montreal Protocol on Substances that Deplete the Ozone Layer, Geneva, Switzerland, 2011.

[21] V. Eyring, D. W. Waugh, G. E. Bodeker et al., "Multimodel projections of stratospheric ozone in the 21st century," *Journal of Geophysical Research D*, vol. 112, no. 16, Article ID D16303, 2007.

[22] T. G. Shepherd, "Dynamics, stratospheric ozone, and climate change," *Atmosphere-Ocean*, vol. 46, no. 1, pp. 117–138, 2008.

[23] D. W. Waugh, L. Oman, S. R. Kawa et al., "Impacts of climate change on stratospheric ozone recovery," *Geophysical Research Letters*, vol. 36, no. 3, Article ID L03805, 2009.

[24] S. Dhomse, M. Weber, I. Wohltmann, M. Rex, and J. P. Burrows, "On the possible causes of recent increases in northern hemispheric total ozone from a statistical analysis of satellite data from 1979 to 2003," *Atmospheric Chemistry and Physics*, vol. 6, no. 5, pp. 1165–1180, 2006.

[25] A. I. Jonsson, J. de Grandpré, V. I. Fomichev, J. C. McConnell, and S. R. Beagley, "Doubled CO_2-induced cooling in the middle atmosphere: photochemical analysis of the ozone radiative feedback," *Journal of Geophysical Research D*, vol. 109, Article ID D24103, 2004.

[26] N. Butchart, A. A. Scaife, M. Bourqui et al., "Simulations of anthropogenic change in the strength of the Brewer-Dobson circulation," *Climate Dynamics*, vol. 27, no. 7-8, pp. 727–741, 2006.

[27] S. J. Eichelberger and D. L. Hartmann, "Changes in the strength of the Brewer-Dobson circulation in a simple AGCM," *Geophysical Research Letters*, vol. 32, no. 15, Article ID L15807, 2005.

[28] D. Hofmann, S. Oltmans, W. Komhyr et al., "Ozone loss in the lower stratosphere over the United States in 1992–1993: evidence for heterogeneous chemistry on the Pinatubo aerosols," *Geophysical Research Letters*, vol. 21, no. 1, pp. 65–68, 1994.

[29] http://toms.gsfc.nasa.gov/.

[30] A. J. Prata and C. Bernardo, "Retrieval of volcanic SO_2 column abundance from Atmospheric infrared sounder data," *Journal of Geophysical Research D*, vol. 112, no. 20, Article ID D20204, 2007.